Magnetic-field-induced phase transitions in singlet magnets with ferromagnetic exchange

V. P. D'yakonov, E. E. Zubov, F. P. Onufrieva, A. V. Saĭko, and I. M. Fita

Odessa State University

Phase transitions in singlet magnets with ferromagnetic exchange were investigated theoretically and experimentally in the presence of an external magnetic field H perpendicular to the "easy plane." The T-H phase diagrams are plotted for different ratios of the one-ion-anisotropy and exchange constants. The order structure is investigated in the spin configurations realized in various ranges of the external parameters. It is shown that only one of the three possible structures is truly ferromagnetic, and the ordering structure at low temperatures in other phases is connected with the quadrupole or with the quadrupole-ferromagnetic order. This causes the magnetic characteristics (magnetization and susceptibility) as functions of the field and temperature to have a unique behavior different from the traditional ferro- and paramagnetic behavior.

1. INTRODUCTION

Singlet magnetism is investigated theoretically and experimentally, using as an example the simplest and at the same time most typical system, a magnet with ferromagnetic exchange and easy-axis one-ion anisotropy (OA), $D(S^z)^2$, $D > 0$. The specific object investigated as nickel fluorosilicate $NiSiF_6 \cdot 6H_2O$, which is a magnetodielectric characterized by isotropic exchange interaction and a uniaxial OA whose constant depends strongly on the pressure and goes through zero at $P = 1.3$ kbar (Ref. 1). At $P > 1.3$ kbar, when $D > 0$, i.e., the ground state of the Ni^{2+} ion is a singlet and the excited state is a degenerate doublet (the node spin is $S = 1$), nickel fluorosilicate is a typical representative of singlet ferromagnets.

Theoretical investigations of such systems date back to the work by Moriya,[2] who introduced a criterion for the existence of ferromagnetism (antiferromagnetism), having shown in the molecular-field approximation that at $D/J_0 > 2$ the ground state in the absence of an external field is nonmagnetic (J_0 is the zeroth Fourier component of the exchange integral). The behavior of such systems was investigated later[3,4] in a magnetic field perpendicular to the "easy plane," and it was shown that the nonmagnetic ground state remains stable in a certain field interval $0 < H < H_{cl}$, while at $H > H_{cl}$ there is restored a cooperative phase, which is ferro- or antiferromagnetic, depending on the sign of the exchange interaction. These predictions were confirmed by experiments[5-9] carried out on Ni compounds characterized by strong OA and weak antiferromagnetic exchange. The theoretical phase diagrams at finite temperatures were constructed in Refs, 4, 10, and 11 for magnets with easy-plane OA in the presence of an external field perpendicular to the easy plane. The possibility of reconstructing the energy spectrum of a magnetic ion from magnetic-measurement results was discussed in Ref. 12.

Interest has increased lately in the study of such systems under conditions when the OA and exchange constants are of the same order.[13-18] It was shown in Ref. 17, in particular, that in this case between these two ordering mechanisms, OA and exchange, leads to the existence of unique types of spin structures at $T = 0$, viz., tensor, tensor-ferromagnetic, and finally ordinary ferromagnetic.

Our purpose here is to investigate the structures of the singlet-ferromagnet spin configurations realized in various temperature and field intervals, of the distinctive features, due to the peculiarities of these structure, of the behavior of the magnetic characteristics, and of the character of the phase transitions (PT) between them. Another aim is to plot the T-H phase diagrams at various ratios of the OA and exchange constants.

The magnetodielectric $NiSiF_6 \cdot 6H_2O$ used for this purpose is an ideal object for the investigation of singlet magnetism. Primarily, it is the first experimentally investigated magnet with strong OA, in which the exchange interaction is ferromagnetic. Next, as established in Ref. 18, the OA constant of this crystal depends strongly on the pressure, so that the D/J_0 can be smoothly regulated and perform the research in the least investigated parameter range which is of greatest interest. (Figure 1 shows the dependence of D/J_0 on the pressure, obtained in Ref. 18 from an analysis of the high-temperature susceptibility measured in a zero field.) The necessary pressure is produced by using the hydrostatic compression method described in detail in Sec. 2. Some preliminary results were reported in Refs. 11 and 19–21.

2. EXPERIMENT

The magnetic properties of nickel fluorosilicate in a magnetic field were measured in a special ^3He-^4He dilution refrigerator,[22] in which the sample could be to cooled to
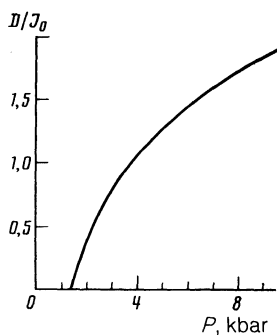
FIG. 1. Pressure dependence of the parameter ratio D/J_0 of nickel fluorosilicate.

0038-5646/87/111013-08$04.00   1013
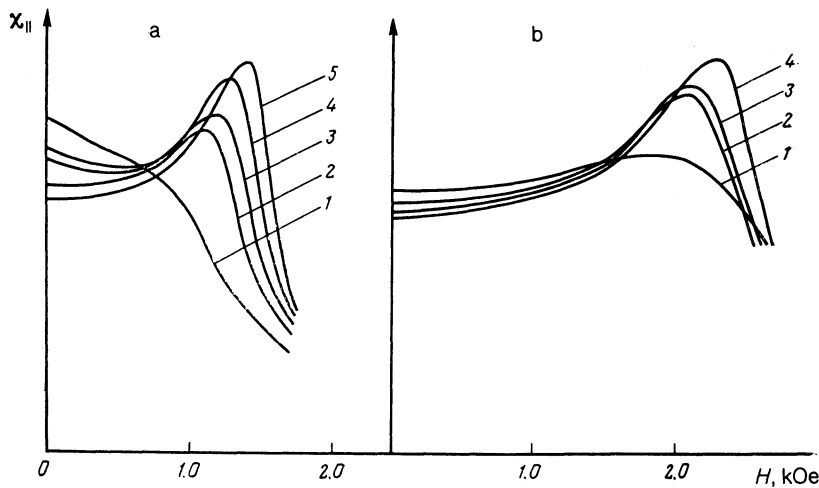
FIG. 2. Experimental field dependence of the longitudinal susceptibility at the following pressures: a) $P = 4.2$ kbar $(D/J_0 = 1.1)$: 1—$T = 181$ mK, 2—124 mK, 3—120 mK, 4—110 mK, 5—103 mK $(T_c(0) = 156$ mK); b) $P = 9.6$ kbar $(D/J_0 = 1.9)$: 1—$T = 168$ mK, 2—132 mK, 3—112 mK, 4—108 mK $(T_c(0) = 114$ mK).

~50 mK. Features of this setup, ensuring simple and convenient operation, are the possibility of placing the sample-containing high-pressure vessel directly in the dilution chamber, and the absence of low-temperature hermetic joints. The temperature in the dilution chamber was stabilized with a heater and determined using Speer carbon thermometers (nominal resistances 100 and 200 Ω) having a negligible magnetoresistive effect in fields up to 5 kOe. The thermometer dc resistance was measured with an RZ003 voltage comparator. The power released by the thermometer did not exceed 10^{-10} W. The temperature error did not exceed 5 mK. A hydrostatic pressure up to 10 kbar was produced in a usual beryllium-bronze chamber of the cylinder + piston type. At helium temperature the pressure was determined accurate to ~0.3 kbar from the temperature of the superconducting transition of single-crystal tin. The magnetic susceptibility of $NiSiF_6 \cdot 6H_2O$ in a constant external magnetic field H was measured by an inductive method using a low-frequency differential magnetometer. The chosen amplitude of the alternating magnetic field h of frequency 30 Hz ranged from 0.3 to 1.0 Oe. The investigated single-crystal sample was a cylinder (1.55 mm diam, $l = 6.0$ mm) with a demagnetization factor $4\pi N \approx 0.7$; the cylinder axis was parallel to the trigonal axis of the crystal. A measuring coil of three pairs of coaxial oppositely wound sections with the $NiSiF_6 \cdot 6H_2O$ and Sn samples were placed in the high-pressure cell. A superconducting solenoid and modulation coils, producing the constant uniform field H and the alternating field h were placed in a ^{4}He bath at 4.2 K. The directions of H and h coincided in the experiment in all cases (accurate to ~3°) with the axis of the cylindrical sample. We measured thus the longitudinal component $\chi_\parallel$ of the susceptibility in a field perpendicular to the easy axis. This is just the field direction that yields the most interesting results, since it will be shown that magnetic structures of three different types are realized then. Inasmuch as we measured in fact the temperature of the thermostat (the dilution bath), much attention was paid to preservation of thermal equilibrium between the sample and the heat bath when the field was turned off. A condition met when plotting $\chi_\parallel(H)$ at constant T was that the field-variation time be longer than the sample thermal relaxation time.

To plot the T-H phase diagram of nickel fluorosilicate we investigated the temperature dependence of the suscepti-

bility in a constant magnetic field and the field dependence of the susceptibility at constant temperatures. These measurements revealed the complicated features of a singlet magnet with ferromagnetic exchange.

Figures 2a and 2b show the experimental field dependences of the susceptibility for two typical pressures, 4.2 kbar $(D/J_0 = 1.1)$ and 9.6 kbar $(D/J_0 = 1.9)$. Whereas at high temperature this dependence is monotonic, at temperatures below some pressure-dependent value of the $\chi_\parallel(H)$ curves exhibit a maximum that shifts, with increase of pressure, towards stronger fields. The fields in which the maximum of $\chi_\parallel(H)$ is observed tend, with decrease of temperature, to a value $D/\mu_B g$ (g is the g-factor and μ_B the Bohr magneton). With increase of temperature, the maximum of the $\chi_\parallel(H)$ curve shifts towards weaker fields and decreases in amplitude. A characteristic feature of the $\chi_\parallel(H)$ depen-
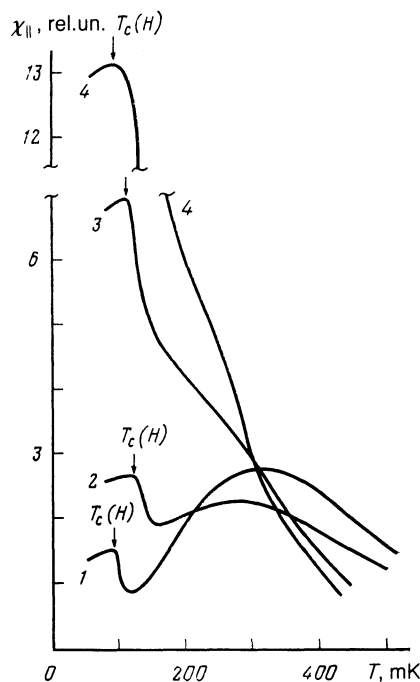
FIG. 3. Experimental temperature dependences of the longitudinal susceptibility in a constant magnetic field at a pressure $P = 9.6$ kbar: 1—$H = 1065$ Oe, 2—1775 Oe, 3—2130 Oe, 4—2660 Oe.

1014   Sov. Phys. JETP 66 (5), November 1987

D'yakonov *et al.*   1014
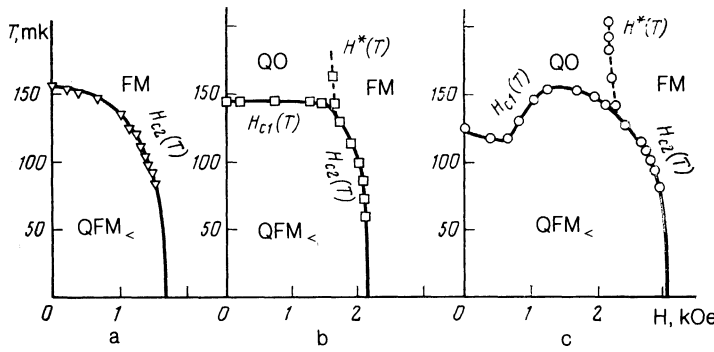
FIG. 4. Experimental $T - H$ phase diagrams of nickel fluorosilicate at various pressures: a—$P = 4.2$ kbar ($D/J_0 = 1.1$), b—7.0 kbar ($D/J_0 = 1.6$), c—8.6 kbar ($D/J_0 = 1.8$).

dence is that at high pressures $P > 7$ kbar (or $D/J_0 > 1.58$) a maximum appears also at temperatures higher than $T_c(0)$ Fig. 2(b).

We analyze now the temperature dependence, obtained from independent experiments, of the longitudinal susceptibility at finite H. Figure 3 shows plots of $\chi_{\parallel}(T)$ for $P = 0.6$ kbar for various magnetic fields. All the curves show a jumplike change of $\chi_{\parallel}(T)$ at a certain temperature $T_c(H)$ that depends on the field strength; this is reminiscent of the behavior of the susceptibility in second-order phase transitions.

Besides the noted jumplike changes of $\chi_{\parallel}(T)$, a smeared maximum, that vanishes with increase of field, is observed in weak field at temperatures $T \approx 250$–350 mk. A rigorous theoretical discussion of the nature of the singularities and maxima of $\chi_{\parallel}(T)$ and $\chi_{\parallel}(H)$ will be carried out in Sec. 3.

Using the experimental field and the temperature dependences of the susceptibilities of NiSiF$_6$·6H$_2$O, we plotted on the T-H plane (Fig. 4) the lines of the maxima of $\chi_{\parallel}(H)$ (the $H_{c2}(T)$ and $H^*(T)$ lines) and the lines of jumplike changes of $\chi_{\parallel}(T)$ ($H_{c1}(T)$ and $H_{c2}(T)$ lines), which coincide on the $H_{c2}(T)$ section within the limits of experimental error. We assume at the present stage that the lines $H_{c1}(T)$ and $H_{c2}(T)$ correspond to second-order phase-transition lines (for the finite-size samples used in the experiments, the susceptibility singularities typical of second-order phase transitions in an infinite crystal broaden into maxima). Besides the closed line $H_{c1}(T) - H_{c2}(T)$ (or, in other words the $T_c(H)$ line), the $T - H$ diagram has a line $H^*(T)$ corresponding to the maxima of $\chi_{\parallel}(H)$ and observed in experiment only at values $D/J_0 \gtrsim 1$. We discuss the nature of these lines in Sec. 3.

The main error of the measured $T_c(H)$ dependence is determined by the deviation of the direction of the constant magnetic field H from the C_3 axis. Unfortunately, it was impossible in our experiment to adjust the orientations of the fields H and h relative to the trigonal axis of the crystal (these difficulties are caused by the experimental conditions—high pressure and infralow temperatures). This made it difficult to obtain exactly reproducible results in different experimental runs at identical parameters H, P, and T. Since the appearance of a weak transverse component of the field H only lowers the phase-transition temperature at fixed values of H(if only a transverse field component is present, there are no phase transitions at all, since the magnetization is parallel to the easy axis for all field values), the phase-transition temperature corresponding to the most ac-

curate orientation $H \parallel C_3$ was taken to be the maximum value of the temperature $T_c(H)$.

To conclude this section, we note that the form of the phase diagrams plotted in accordance with the positions of the maxima of (T) at constant H and of $\chi_{\parallel}(H)$ at constant T depend substantially on the ratio of the OA and exchange constants. These phase diagrams have the standard form typical of a ferromagnet with easy-plane exchange anisotropy at small D/J_0 and acquire new qualitative features when D/J_0 is increased. In particular, for $D/J_0 \gtrsim 1.6$ the $T_c(H)$ plot rises in the weak-field region, while near the critical value $D/J_0 = 2$ (at which $T_c(0)$ vanishes) the phase diagram is abruptly restructured at small H, so that even an insignificant change of D/J_0 leads to an appreciable change of $T_c(H)$ for weak H.

3. THEORY

Nickel fluorosilicate, a magnetodielectric with isotropic ferromagnetic exhange and easy-plane anisotropy,[1,17] placed in a magnetic field perpendicular to the easy plane, is described by the Hamiltonian

$$\mathcal{H} = -\frac{1}{2}\sum_{ij}J_{ij}(\mathbf{S}_i\mathbf{S}_j) + D\sum_i(S_i^z)^2 - H\sum_i S_i^z, \quad D > 0. \quad (1)$$

We construct the theoretical phase diagram by using the microscopic theory [15–17] developed for the description of the dynamic properties of magnetic dielectrics of arbitrary symmetry and OA intensity. We confine ourselves in the present paper to the zeroth approximation of the self-consistent-field (SCF) theory. In this approximation Hamiltonian takes the form

$$\mathcal{H}_0 = -(J_0\langle S^z\rangle + H)\sum_i S_i^z - J_0\langle S^x\rangle\sum_i S_i^x + D\sum_i(S_i^z)^2. \quad (2)$$

It is reduced, by the unitary SU(3)-group transformation described in detail in Ref. 15, to the diagonal form

$$\tilde{\mathcal{H}}_0 = -\tilde{h}\sum_i \tilde{S}_i^z + \tilde{d}\sum_i[(\tilde{S}_i^z)^2 - \tfrac{2}{3}], \quad (3)$$

where the effective fields are equal to

$$\tilde{h} = \tilde{H}\cos 2L - \tilde{D}_2\sin 2L,$$

$$\tilde{d} = \tfrac{1}{2}D(3\cos^2 K\cos^2\varphi - 1)$$
$$- \tfrac{3}{2}H\sin\varphi\sin 2K - \tfrac{3}{4}J_0\sin^2 2K(\lambda + \sigma\sin 2L), \quad (4)$$

$$\tilde{H} = H\cos\varphi\cos K - \tfrac{1}{2}D\sin 2\varphi\sin K + J_0\sigma\cos^2 K\cos 2L,$$

$$\tilde{D}_2 = -\tfrac{1}{2}H\sin\varphi\sin 2K + \tfrac{1}{2}D(\cos^2 K\cos^2\varphi - \cos 2\varphi)$$
$$- \tfrac{1}{4}J_0\sin^2 2K(\lambda + \sigma\sin 2L)$$

(the tilde labels operators connected with the initial operators by the indicated unitary transformations).

For the angles φ, K, and L, of the unitary transformation we have the equations

$$\tfrac{1}{2}D \sin 2\varphi \cos K + H \cos \varphi \sin K + \tfrac{1}{2}J_0 \sigma \sin 2K \cos 2L = 0,$$

$$\tfrac{1}{2}D \cos^2 \varphi \sin 2K + H \sin \varphi \cos 2K$$
$$+ \tfrac{1}{4}J_0 \sin 4K (\lambda + \sigma \sin 2L) = 0, \qquad (5)$$
$$\tilde{H} \sin 2L + \tilde{D}_2 \cos 2L = 0.$$

They contain the mean values $\sigma = \langle \tilde{S}^z \rangle$ and $\lambda = \langle \tilde{O}_2^0 \rangle$ defined by the transcendental equations

$$\sigma = \exp(-\tilde{d}/\Theta)2 \operatorname{sh}(\tilde{h}/\Theta)[1 + \exp(-\tilde{d}/\Theta)2 \operatorname{ch}(\tilde{h}/\Theta)]^{-1},$$
$$\lambda = 1 - 3[1 + \exp(-\tilde{d}/\Theta)2 \operatorname{ch}(\tilde{h}/\Theta)]^{-1}, \quad \Theta = k_B T. \qquad (6)$$

The five quantities φ, K, L, σ, λ, obtained by explicit solution of the set equations (5) and (6) determine uniquely the structure of the spin order and the equilibrium magnetic properties of the considered magnetodielectric. In particular, the structure of the spin order is determined by the eight-dimensional order parameter (OP) η introduced in Ref. 17, whose independent components are the spin and quadrupole components $\langle S^\alpha \rangle$ $(\alpha = +, -, z)$ and $\langle O_2^m \rangle$ $(m = 0, \pm 1, \pm 2)$.[1] The spin components, i.e., the magnetizations, are connected here with the indicated five quantities by the relations

$$M_\| \equiv \langle S^z \rangle = \sigma \cos 2L \cos \varphi \cos K + \tfrac{1}{2} \sin \varphi \sin 2K (\lambda + \sigma \sin 2L), \qquad (7)$$

$$M_\perp \equiv \langle S^x \rangle = \sigma \cos 2L \sin \varphi \cos K - \tfrac{1}{2} \cos \varphi \sin 2K (\lambda + \sigma \sin 2L),$$

and the quadrupole components $Q_0 \equiv \langle 3O_2^0 \rangle$, $Q_2 \equiv \langle O_2^2 + O_2^{-2} \rangle$, and $Q_1 \equiv \langle O_2^1 - O_2^{-1} \rangle$ are related by Eqs. (13) of Ref. 15. The absolute value of the order parameter is[17]

$$\eta = (\sigma - \lambda)/2, \qquad (8)$$

and its orientation in spin-quadrupole space is determined by the direction cosines that are connected with $\varphi, K, L, \sigma, \lambda$ by Eqs. (9) and (11) of Ref. 17. Equations (7) for the magnetizations make it also possible to calculate the longitudinal and transverse components of the susceptibility

$$\chi_\| = \partial M_\| / \partial H, \quad \chi_\perp = \partial M_\perp / \partial H, \qquad (9)$$

by numerical or analytic differentiation.

We point out that, according to Eqs. (6), three variants of solutions are possible for σ and λ:

$$\sigma = 0, \quad \lambda = -2, \qquad (10a)$$
$$\sigma = 1, \quad \lambda = 1, \qquad (10b)$$
$$\sigma = -1, \quad \lambda = 1. \qquad (10c)$$

Each corresponds to different values of the angles given in (5). This means the possibility of having that three types of local coordinates (coordinates in which the zeroth Hamiltonian is diagonal) determined, naturally, by different "generalized Euler angles" φ, K, and L (see Ref. 17 for details). It is convenient to fix the type of local frame and use these coordinates to describe the possible ordered phases and the phase transitions between them. We use in the present paper coordinates in which $\sigma(T = 0) = 0$ and $\lambda(T = 0) = -2$.

Let us investigate the solutions of the system (5) for arbitrary T. There are three different solution branches. Two are trivial solutions determined by the angles

$$\sin \varphi = \sin 2K = \sin 2L = 0, \qquad (11)$$
$$\cos \varphi = \cos 2K = \cos 2L = 0. \qquad (12)$$

The third solution is described for $T = 0$ by the equation

$$\cos 2K = \xi[1 - (H/D)^2], \quad \sin \varphi = -(H/D)\{[1/\xi - 1 + (H/D)^2]/[1/\xi + 1 - (H/D)^2]\}^{1/2}, \qquad (13)$$
$$\operatorname{tg} 2L = -\tilde{D}_2/\tilde{H}, \text{where } \xi \equiv D/2J_0,$$

and can be described for finite T only numerically. It is important that in the latter, in contrast to the solutions (11) and (12), the angles are smooth functions of the Hamiltonian parameters H, D, and J_0.

It is easy to verify that the nontrivial solution corresponds to a canted ferromagnetic structure $M_\| \neq 0$, $M_\perp \neq 0$, while the trivial solutions correspond to collinear structures ($m_\perp = 0$). The latter are substantially different at $T = 0$. Solution (12) corresponds to a structure with $M_\| = 1$ and $M_\perp = 0$, i.e., to a saturated ferromagnetic structure, while solution (11) corresponds to a structure with $M_\| = M_\perp = 0$. For a nonmagnetic structure we have here $Q_0 = -2$, which corresponds to presence of quadrupole order when all the spins are located in a plane perpendicular to the z axis.[2]

This symmetry difference between the structure vanishes at finite temperatures: in both cases the longitudinal magnetization component $M_\|$ and the quadrupole mean value Q_0 differ from zero. The difference is that the dominant contribution to the eight-dimensional order parameter is made by the ferromagnetic components (FM structure) in one case and in the quadrupole components (QO structure) in the second.

The foregoing is easily understood by analysis in a somewhat different language, in particular, by analyzing the level scheme relative to an individual ion in the molecular field. For the solutions (11) and (12) the levels can be numbered by the projections of the spin on the z axis. In this case the solution (12), i.e., the FM structure, corresponds to the usual scheme, in which the lowest is the level with maximum projection, $|1\rangle$ in this case. For solution (11), i.e., for the QO structure, the lowest is the nonmagnetic $|0\rangle$ level. The first of these level schemes corresponds to the relation $M_\| > -Q_0$ between the ferromagnetic and quadrupole components of the order parameter, and the second to $M_\| < -Q_0 (Q_0 < 0)$. The condition

$$M_\| = -Q_0 \qquad (14)$$

corresponds to crossing of the levels $|0\rangle$ and $|1\rangle$. The line on which this condition is met (it will be shown below to be the $H^*(T)$ line on the phase diagram of Fig. 5) is a line of additional degeneracy, with the system having effectively only two levels.

A nontrivial solution requires in addition to nonzero components $M_\|$ and Q_0 (the mean values of the diagonal spin and quadrupole operators) also the components $M_\perp$, Q_1, and Q_2, which are the mean values of the off-diagonal spin and quadrupole operators. The reason is the spontaneous loss of symmetry with respect to three-dimensional rotations about the z axis in the corresponding structure, which
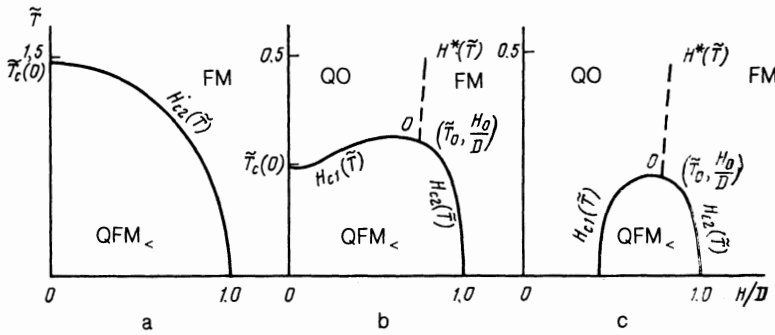
FIG. 5. Theoretical $T - H$ phase diagrams of nickel fluorosilicate at different values of the parameter D/J_0: a—$D/J_0 = 0.5$; b—1.9; c—2.5. The $H_{c1}(T)$ line corresponds to the phase boundary (15), $H_{c2}(T)$ to the phase boundary (16), and $H^*(T)$ to the boundary (19a).

we shall name angular quadrupole-ferromagnetic (QFM$_<$). A nonzero component $M_\perp$ makes it impossible to number the levels of an ion in the molecular field in terms of the spin projections along the z axis, so that no simple qualitative analysis similar to the carried out above is possible. It can only be noted that in a QFM$_<$ structure the relative contribution of the quadrupole and ferromagnetic components to the order parameters varies with the parameters T, H, and D. In particular, the contribution of the quadrupole components is a maximum on the phase boundary with the QO phase and a minimum on the boundary with the FM phase (see the theoretical phase diagram in Fig. 5).

We procede now to describe the construction of the theoretical phase diagrams. A nontrivial solution exists in a bounded region of the parameters H, D, and T. On the boundaries of this region the angles take on values corresponding to the trivial solutions (11) or (12). These respective boundaries can be determined after eliminating from the system (5) the trivial solutions and substituting the condition that the angles be equal to their values (11) and (12).

The boundary determined in this manner, where the angles take on values corresponding to the QO solution (11), is described by the equation

$$D^2 - H(H - J_0\sigma) + DJ_0\lambda = 0, \tag{15}$$

in which σ and λ are determined by Eqs. (6) with $\sin\varphi = \sin K = \sin 2L = 0$, while the boundary where the angles take on values corresponding to the FM solution (12) is described by the equation

$$2DJ_0\sigma - (H - D)[H + D - \tfrac{1}{2}J_0(\lambda + \sigma)] = 0, \tag{16}$$

in which σ and λ are determined by Eqs. (6) in which $\cos\varphi = \cos 2K = \cos 2L = 0$ is substituted.

On the other hand, the trivial solutions (11) and (12) exist for all D, T, and H. They are expected to be stable only in a certain region of the T-H plane. The instability lines can be obtained by investigating the spectrum of the collective excitations of structures corresponding to the solutions (11) and (12), as lines of relaxation of the lower-lying mode. Equations for the corresponding spectra can be obtained from Eqs. (35) and (36) of Ref. 16, where a dispersion equation is given for arbitrary φ, K, and L in the zeroth approximation in the reciprocal of the exchange-interaction radius for the irreducible part of the diagram. Substituting the values of the angles (11) and (12), we obtain respectively for the low-lying branch of the QO spectrum

$$\omega_{QO}(\mathbf{k}) = [D^2 + DJ_k\lambda + (J_k\sigma/2)^2]^{1/2} - (H - J_0\sigma + J_k\sigma/2) \tag{17}$$

and for the low-lying branch of the FM structure

$$\omega_{FM}(\mathbf{k}) = \{[H - (2J_0 - J_k)(\lambda + \sigma)/4]^2 + J_k^2\sigma(\sigma - \lambda)/2\}^{1/2} - [D + J_k\sigma/2 + J_k(\sigma - \lambda)/4] \tag{18}$$

(J_k is the Fourier transform of the exchange integral and $\mathbf{k}$ is the quasimomentum).

It is easily verified that the equations for the stability boundaries of each of the collinear structures, determined by the conditions $\omega_{QO}(0) = 0$ and $\omega_{FM}(0) = 0$, are equal respectively to Eqs. (15) and (16)—the lines $H_{c1}(T)$ and $H_{c2}(T)$ in Fig. 5 are lines of second-order phase transitions between the QO and QFM$_<$ and between the QFM$_<$ and FM structures, respectively. It follows from Eqs. (7), (11), and (12) of the present paper and from Eqs. (13) of Ref. 15 that three off-diagonal components $M_\perp$, Q_1, and Q_2 of the order parameter vanish on these lines; the longitudinal magnetization $M_\parallel$ and the quadrupole mean value A_0 have kinks, while the susceptibilities have irregularities in the form of a jump of the longitudinal component $\chi_\parallel$ and of a singularity of the off-diagonal component $\chi_\perp \sim |H - H_{ci}|^{-1/2}(i = 1,2)$.

Note that the condition $M_\parallel < -Q_0(Q_0 < 0)$ which, as noted above, is in general typical of the QO structure, is satisfied on the entire $H_{c2}(T)$ line, while the condition $M_\parallel > -Q_0$, which is typical of the FM structure, is met on the H_{c2} line. Since we wish to determine the coordinates of the phase-diagram point O at which $H_{c1}(T) = H_{c2}(T)$, we put $M_\parallel = -Q_0$ or, the relation $\sigma = \lambda$ equivalent at the angle values (11) and (12). It is easy to verify, however, that under this condition the equations (15) and (16) for the phase boundaries are identically equal and can take the form

$$H - J_0\sigma - D = 0 \tag{19}$$

or, explicitly,

$$H = D - J_0[1 - \exp(-2/\tilde{T})]/[2 + \exp(-2/\tilde{T})], \tilde{T} = k_B T/D. \tag{19a}$$

It can be simultaneously seen from (6) that Eq. (19) is precisely the condition for satisfaction of the equality $\sigma = \lambda$. This is readily verified by calculating the effective fields $\tilde{h}$ and $\tilde{d}$ in Eq. (6) for the angle values (11) and (12). Thus, Eqs. (15) and (16) describe not only the lines $H_{c1}(T)$ and $H_{c2}(T)$ but no more line, (19a), shown dashed in Fig. 5 and labeled $H^*(T)$.

The coordinates of the intersection point O of the lines $H_{c1}(T)$, $H_{c2}(T)$ and $H^*(T)$ can be determined from the explicit forms of the equations for the phase line $H_{c1}(T)$ or $H_{c2}(T)$ for small $\sigma - \lambda$, when these equations take the form $\tilde{T} = [2\xi(H/D + 1)]^{-1}$, and substituting in (19a). As a re-

sult we obtain for the temperature at this point, which we designate T_0, the equation

$$2 - \frac{1}{2\xi} \frac{1 + 2/\tilde{T}_0 - \exp(-2/\tilde{T}_0)}{2 + \exp(-2/\tilde{T}_0)} = 0, \qquad (20)$$

and for the corresponding field we have

$$H_0/D = 1/2\xi\tilde{T}_0 - 1. \qquad (21)$$

In constrast to the lines $H_{c1}(T)$ and $H_{c2}(T)$, $H*T$ is not a phase-transition line, since there is no symmetry difference between the QO and FM structures at finite temperatures. This line, however, separates structures with qualitatively different behavior of a number of properties as functions of the field at $T = $ const. For example, the longitudinal susceptibility $\chi_\parallel(H)$ increases with increase of H in the QO phase and decreases in the FM phase (see Fig. 7), the frequency of the lowest mode decreases with increase of H in the QO phase and increases in the FM phase [see Eqs. (17) and (18)], and so on. This makes $H*(T)$ the line of the maxima of $\chi_\parallel(H)$, the line where the frequencies of the ferromagnetic resonance vanish, etc. The reason for this circumstance is that the degree of ordering in the system at a fixed temperature increases symmetrically in both directions on moving away from the indicated line; in particular, the quadrupole order increases and the ferromagnetic order decreases when the field decreases. The absolute value of the order parameter, which characterizes the aggregate order in the system and is given by Eq. (8) turns out to be zero on this line.

Although the absolute value of the order parameter increases symmetrically on both sides of the indicated line, the predominance of the different types of ordering in the QO and FM phases leads to a qualitatively different behavior of the measured quantities (the magnetization and the static magnetic susceptibility) as functions of T at fixed H, since these quantities characterize only one subsystem. In particular, a feature of fields belonging to the FM structure is the traditional behavior of a ferromagnet at $T > T_c(H)$, namely
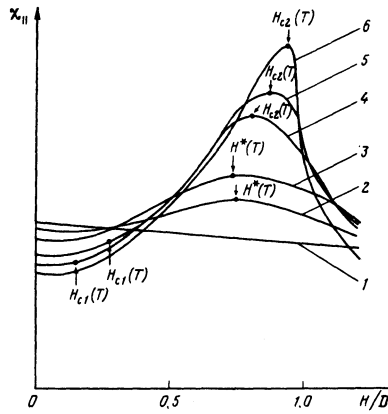
FIG. 7. Theoretical field dependences of the longitudinal susceptibility for the case $D/J_0 = 1.9$ ($\tilde{T}_0 = 0.303$): 1—$\tilde{T} = 1,0$; 2—0.45; 3—0.38; 4—0.28; 5—0.26; 6—0.2; 1-3—$\tilde{T} > \tilde{T}_0$, 4-6—$\tilde{T} < \tilde{T}_0$.

the montonic decrease of the longitudinal magnetization and of the longitudinal susceptibility with increase of T at constant H (see curves 3 and 4 in Figs. 6a and 6b). On the contrary, fields where a QO structure exists, and at values of H not too close to $H*(T)$, are have at $T > T_c(H)$ values of $M_\parallel$ and $\chi_\parallel$ that depend anomalously on T, first increasing with increase of T, passing through a maximum, and only then begin to decrease (see curves 1 and 2 in Figs. 6a and 6b). The quantities that characterize the spin order on the whole, the absolute value of the order parameter η, and the generalized susceptibility $\chi = \partial\eta/\partial\tilde{h}$ have a traditional behavior and decrease with T at $T > T_c(H)$ for all values of the parameter H.

As shown by the calculations, the indicated differences in the behavior of $M_\parallel(T,H)$ and $\chi_\parallel(T,H)$ in QO and FM structures manifest themselves at sufficiently low relative temperatures $T \lesssim 0.7$, and vanish at higher T (see, e.g., curve 1 of Fig. 7 for $T = 1.0$, on which there is no maximum of $\chi_\parallel(H)$, and therefore do not exist at all at $D/J_0 \lesssim 1.05$, when the entire paramagnetic phase is in the region of higher T. The reason is that as the temperature is increased the thermal fluctuations weaken both types of disorder, ferromagnetic and quadrupole, the difference between the QO and FM structures decreases, and their properties approach those of an ordinary paramagnet. We have discussed in so much detail the cause of the $H*(T)$ line and some of the features of the properties connected with its existence, because ignorance of these features may impede the interpretation of the experimental data, as will be shown in the next section.

4. COMPARISON OF EXPERIMENTAL AND THEORETICAL RESULTS. CONCLUSIONS

We turn now to an interpretation of the experimental data and to a comparison of the experimental and theoretical susceptibility curves. In experiments, the locations of the second-order phase transition points at finite H are determined from the behavior of the longitudinal susceptibility $\chi_\parallel(H)$. For samples of infinite size, this quantity should change jumpwise at phase-transition points. For finite sample dimensions, as in experiment, the jump is smeared out and the phase-transition points are actually determined from the positions of the $\chi_\parallel(H)$ maxima. If this procedure is used to construct the phase diagrams in our case, we obtain

FIG. 6. Theoretical temperature dependences of the longitudinal magnetization and of the longitudinal susceptibility for the case $D/J_0 = 1.9$. The figure shows the dimensionless quantities $M_\parallel$ and $\chi_\parallel$ defined by Eqs. (7) and (9): 1—$H/D = 0.3$; 2—0.4; 3—0.8; 4—0.9; 1, 2—$H < H_0$; 3, 4—$H > H_r$ and $D/J_0 = 1.9$ $H_0/D = 0.73$).

the picture given in Ref. 20, where preliminary experimental results were published, i.e., we get a phase line consisting of two sections, $H_{c2}(T)$ and $H^*(T)$. The position of the $H_{c1}(T)$ line is not determined in this case.

According to the developed theoretical premises, the $H^*(T)$ line drawn in this manner is not a phase-transition line, and the nature of the $\chi_{\parallel}(H)$ maxima on it was explained in Sec. 3. On the other hand, the theory predicts the existence of $\chi_{\parallel}(H)$ jumps on both the $H_{c2}(T)$ and the $H_{c1}(T)$ lines. Why are the latter not determined in experiment? The reason became clear after the theoretical plots of $\chi_{\parallel}(H)$ were obtained (see Fig 7). It turns out that at the points $H = H_{c1}(T)$ the numerical values of the jumps are very small and, most importantly, they appear above a background, a smooth monotonically increasing section of the $\chi_{\parallel}(H)$ curves, whereas at the points $H = H_{c2}(T)$ the jumps are above the background of a plot of $\chi_{\parallel}(H)$ that is as a whole nonmonotonic. This makes it impossible to determine these jumps and accordingly the H_{c1} line is determined in experiment by measuring $\chi_{\parallel}(H)$ at constant T.

On the other hand, the $H_{c1}(T)$ line can be recorded by measuring $\chi_{\parallel}(T)$ at fixed H (see Fig. 6b). The same measurements yield also the $H_{c2}(T)$ line, whose position coincides, as it should, with the position determined by measuring $\chi_{\parallel}(H)$.

As a result we obtain the experimental phase diagrams shown in Fig. 4 for different D/J_0. When comparing the experimental and theoretical phase diagrams, notice must be taken of the characteristic transformation, in both types of closed phase-transition line, of $T_c(H)$ from a monotonically decreasing plot in the case $D/J_0 \ll 1$, the same as for a ferromagnet with exchange anisotropy, to a strongly nonmonotonic one at $D/J_0 \sim 1$ (see the experimental, Fig. 4, and theoretical, Fig. 5, phase diagrams). The case of intermediate values of D/J_0 is particularly interesting. It corresponds at first glance to the situation standard for an easy-plane ferromagnet: in the absence of low T there is realized a ferromagnetic phase with a magnetization oriented parallel to the easy plane, which goes over next with increase of T into a nonmagnetic phase via a second-order phase transition at $T = T_c$. At intermediate D/J_0, however, the phase line is transformed in such a way that it becomes possible at $T > T_c(0)$ to restore cooperative order in the easy plane when the field is applied along the "difficult axis." The reason lies in the more complicated phase structure, described in detail in Sec. 3.

To determine the theoretical value of $(D/J_0)^*$, at which a restructuring of the character of the plane lines takes place, namely, the appearance of an increasing section of $T_c(H)$, we write down the equation that follows from (15) for $T_c(H)$ at small H:

$$[\tilde{T}_c(H)]^{-1}-[\tilde{T}_c(0)]^{-1}=\alpha C(H/D)^2, \qquad (22)$$

where

$$C = \frac{(2J_0-D)(J_0+D)\alpha/6\tilde{T}_c^2(0)-D}{(2J_0-D)(J_0+D)/3}$$

$$\alpha = \frac{3D}{3D-(2J_0-D)/\tilde{T}_c(0)}, \qquad [\tilde{T}_c(0)]^{-1}=\ln\left[\frac{2(J_0+D)}{2J_0-D}\right].$$

The value of $(D/J_0)^*$ is determined from the condition $C = 0$ and turns out to equal 1.48. Note that this value agrees
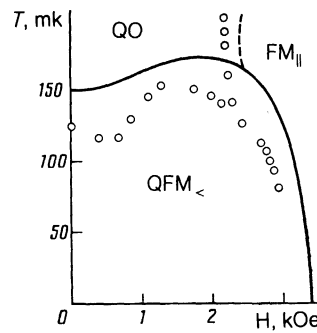
FIG. 8. Comparison of the experimental and theoretical $T - H$ phase diagrams for the case $P = 8.6$ kbar $(D/J_0 = 1.8)$: points—experiment, solid curve—theory.

well with the experimental $(D/J_0)^* = 1.58$.

As a whole, the quantitative comparison of the experimental and theoretical phase diagrams for the most typical experimental case $(D/J_0)^* = 1.8$ $(P = 8.6)$ kbar is shown in Fig. 8.

Summarizing briefly the features of the phase diagrams and phase transitions in ferromagnets with easy-plane one-ion anisotropy in cases when $D \sim J_0$ and $S = 1$, compared with the semiclassical limiting case $D/J_0 \ll 1$ or $S \gg 1$, we note the following.

1. The existence of three structures (QO), QFM$_<$, and FM) rather than two in the indicated semiclassical cases leads to a characteristic form of the phase diagrams and to their unusual transformation with change of D/j_0.

2. At low temperatures $(T < T_0)$ the phase transitions with respect to field between these structures are of second order. At high temperatures $(T > T_0)$ the transitions between the QO and FM structures are smooth.

3. A feature of the QO structure is an anomalous behavior of the longitudinal magnetization and of the longitudinal susceptibility as functions of T, particularly their growth with temperature at $H = $ const in a certain region of temperatures T. This behavior goes over into the standard "paramagnetic" behavior with further increase of T. Since it is connected with the unusual structure of the order, one should expect also an unusual behavior of other magnetic properties.

4. In the paramagnetic region there exists a certain line, $H^*(T)$, on which the character of the dependence of a number of quantities on H varies. This variation was observed in the present experiment for the longitudinal susceptibility $\chi_{\parallel}(H)$, which has a maximum at $H = H^*(T)$. Similar variations of other quantities, such as the ferromagnetic-resonance frequencies, are predicted.

[1] The tensor operators O_m^2 are defined in Ref. 15 viz., $O_2^0 = (S^z)^2 - 1/3S(S+1), O_{\pm}^{\pm 1} = -(S^zS^{\pm} + S^{\pm}S^z), O_{\pm}^{\pm 2} = (S^{\pm})^2$.

[2] The quadrupole mean value Q_0 is so defined that $Q_0 = 0$ for a random disposition of the spins $(\langle(S^z)^2\rangle = \langle(S^x)^2\rangle = \langle(S^y)^2\rangle = 2/3$. $Q_0 = 2$ in the case of complete quadrupole order $(\langle(S^z)^2\rangle = 0$, and $Q_0 = 1$ for complete ferromagnetic order along the z axis $(\langle(S^z)^2\rangle = 1$.

[1] V. G. Bar'yakhtar, I. M. Vitebskiĭ, A. A. Galkin, et al., Zh. Eksp. Teor. Fiz. 84, 1083 (1983) [Sov. Phys. JETP 57, 628 (1983)].
[2] T. Moriya, Phys. Rev. 117, 635 (1960).
[3] T. Tsuneto and T. Murao, Phsica (Utrecht) 51, 186 (1971).
[4] C. Isikawa and Y. Endo, J. Progr. Theor. Phys. 55, 650 (1976).
[5] R. L. Carlin and V. Van Duyneveldt, J. Acc. Chem. Res. 13, 231 (1980).

[6]I. J. Smit, L. I. de Jongh, D. de Klerk, *et al.*, Physica (Utrecht) **86**, 1147 (1977).

[7]W. G. Bos, T. O. Klassen, N. J. Poulis, and R. L. Carlin, J. Magn. and Magn. Mater. **15–18**, 464 (1980).

[8]N. Wada, K. Amaja, and T. Hasaeda, J. Phys. Soc. Jpn. **43**, 341 (1977).

[9]H. A. Algra, J. Barotholome, L. I. de Jongh, *et al.* Physica (Utrecht) **93**, 35 (1978).

[10]Yu. V. Pereverzev and V. G. Borisenko, Fiz. Teverd. Tela (Leningrad) **26**, 1249 (1984) [Sov. Phys. Solid State **26**, 762 (1984)].

[11]F. P. Onufrieva, *ibid.* p. 3435 [2062].

[12]E. Zavadskiĭ, Proc. All-Union Seminar on Magnetic Phase Transitions and Critical Phenomena, Makhachkala, 1984, p. 131.

[13]V. M. Loktev and V. S. Ostrovskiĭ, Fiz. Tverd. Tela (Leningrad) **20**, 3086 (1978) [Sov. Phys. Solid State **20**, 1779 (1978)].

[14]V. M. Loktev and V. S. Ostrovskiĭ, *ibid.* **21**, 3559 (1981) [**21**, 2054 (1981)].

[15]F. P. Onufrieva, Zh. Eksp. Teor. Fiz. **80**, 2372 (1981) [Sov. Phys. JETP **53**, 124 (1981)]. Fiz. Tverd. Tela (Leningrad) 23, 2664 (1981) [Sov. Phys. Solid State **23**, 1562 (1981)].

[16]F. P. Onufrieva, Zh. Eksp. Teor. Fiz. **86**, 1691 (1981) [Sov. Phys. JETP **59**, 986 (1984)].

[17]F. P. Onufrieva, *ibid.* **89**, 2270 (1985) [**62**, 1311 (1985)].

[18]V. P. D'yakonov, G. G. Levchenko, I. M. Fita, and G. A. Tsintsaxse, *ibid.* **87**, 2193 (1984) [**60**, 1268 (1984)].

[19]V. P. D'yakonov and P. M. Fita, in Ref. 12, p. 44.

[20]V. P. D'yakonov and I. M. Fita, Fiz. Tverd. Tela (Leningrad) **25**, 3478 (1983) [Sov. Phys. Solid State **25**, 2003 (1983)].

[21]F. P. Onufirieva, in Ref. 12, p. 84.

[22]V. P. D'yakonov and I. M. Fita, Prib. Tekh. Eksp. No. 6, 238 (1984).

Translated by J. G. Adashko

1020   Sov. Phys. JETP **66** (5), November 1987

D'yakonov *et al.*   1020